

Antiferroelectric Chiral Smectic- O^* Liquid Crystal

Yves Galerne

*Groupe des Matériaux Organiques, Institut de Physique et Chimie des Matériaux de Strasbourg,
Institut Charles Sadron, 6, rue Boussingault, 67083 Strasbourg CEDEX, France*

Lionel Liebert

Laboratoire de Physique des Solides, Université Paris-Sud, 91405 Orsay, France

(Received 29 January 1991)

A macroscopic study of chiral smectic- O^* films, which float at the free surface of isotropic droplets of 1-(methyl)-heptyl-terephthalidene-bis-amino cinnamate, is presented. It allows us to directly prove antiferroelectricity with in-plane polarization in the smectic- O^* phase, and to confirm the herringbone structure of this original phase. The bulk antiferroelectric polarization is measured to be about 0.1 D per molecule.

PACS numbers: 61.30.Eb, 61.30.Gd, 64.70.Md, 68.15.+e

A few years ago, Levelut *et al.*¹ discovered a new liquid-crystal phase that they called the smectic- O phase (Sm- O), in 1-(methyl)-heptyl-terephthalidene-bis-amino cinnamate (MHTAC). They showed that this new phase greatly resembles the smectic- C phase (Sm- C), with the molecules positionally disordered inside the layers, and tilted relative to them ($\psi \approx 50^\circ$). As recently shown in the racemic compound, the difference from Sm- C is that the tilt occurs in alternate directions from one layer to another, forming a *herringbone* structure.² MHTAC is a chiral molecule. It also allows one to observe the chiral Sm- O^* phase¹ in which each individual smectic layer is equivalent to a small ferroelectric Sm- C^* sample. The Sm- O^* layers therefore bear a permanent electric polarization parallel to the layer, which *alternates* from one layer to another. The symmetry of the chiral Sm- O^* phase, which is that of an alternate Sm- C^* phase, thus explains its recently observed *antiferroelectric* in-plane polarization.³ Also, almost simultaneously, a similar antiferroelectric phase with in-plane polarization has been proposed on the basis of rather indirect measurements in 4-(1-methylheptyloxy carbonyl)-phenyl 4'-octyloxybiphenyl-4-carboxylate.⁴ Notice that such an antiferroelectricity is of a different nature from the antiferroelectricity previously discovered in the smectic- A_2 , smectic- A_d , and smectic- A phases of strongly polar compounds.⁵ In these cases, the antiferroelectric polarization is perpendicular to the smectic layers.

In this Letter, we report direct electric measurements on the Sm- O^* phase of chiral MHTAC, which definitely prove the antiferroelectricity of this phase. In addition, this study reinforces the herringbone model proposed for the Sm- O phase in Ref. 2.

The measurements are performed on the Sm- O^* film which floats at the free surface of MHTAC droplets heated in the isotropic phase (Iso) [Fig. 1(a)]. Such a smectic film is currently observed at the free surface of isotropic liquid crystals.⁶ It grows epitaxially in a layer-by-layer fashion when the isotropic droplet is slowly cooled down, each new smectic layer being pretransitionally induced by surface long-range forces at the smectic-air interface. With MHTAC, the smectic film is able to

grow in this manner without any limitation when approaching the isotropic to smectic- O^* transition temperature of the bulk ($T_c = 132^\circ\text{C}$ for the chiral compound). The number of smectic layers in the film is related to temperature by the power law $N \propto (T - T_c)^{-1/3}$. This behavior is due to the van der Waals nature of the interactions of the molecules with the surface.⁷ It allows one to tune the sample thickness by means of temperature.²

Figure 1 depicts the structure of the Sm- O^* film: in the y - z plane, perpendicular to the film and containing the molecules of the first layer in contact with the air [Fig. 1(a)]; and in the x - y plane of the film [Figs. 1(b) and 1(c)]. \mathbf{m}_i is the director of the i th layer, defined by

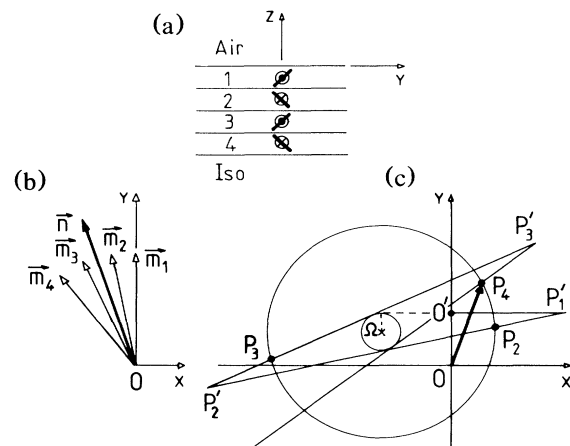


FIG. 1. Structure of a four-layer Sm- O^* film floating at the air-isotropic interface of a MHTAC droplet. The layers are numbered according to their formation order with decreasing temperature, i.e., from the air to the isotropic phase. The last layer (here number 4) is in reality about twice the thickness of the others, and most probably in the nematic phase (see text). For the sake of simplicity, this detail is not taken into account in the drawing. (a) Vertical cut showing the herringbone arrangement of the molecules and the antiferroelectric in-plane polarizations. (b),(c) Horizontal projections of the constructions of the director \mathbf{n} and of the polarization \mathbf{OP}_4 of the Sm- O^* film, respectively. (Not to scale.)

the projection of its molecules onto the film. $\mathbf{n} = \langle \mathbf{m} \rangle$ is the director of the whole film. The structure of the Sm- O^* film is alternate and helicoidal; each layer director \mathbf{m}_i is rotated by a constant angle ω relative to its neighboring-layer director. The Sm- O^* layers, moreover, being individually equivalent to small Sm- C^* samples, bear a permanent ferroelectric polarization perpendicular to \mathbf{m} and parallel to the film. These electric polarizations are represented in Fig. 1(c) by geometrical vectors of equal modulus, $\mathbf{P}'_1\mathbf{P}'_2$ for the second layer, $\mathbf{P}'_2\mathbf{P}'_3$ for the third layer, etc., successively rotated by $\pi + \omega$. Because of surface effects, the first and last layers, at least, support different, and probably reduced, ferroelectric polar-

izations represented by $\mathbf{O}'\mathbf{P}'_1$ and $\mathbf{P}'_{N-1}\mathbf{P}'_N$, respectively. In addition to the ferroelectric contribution, the first layer, as in the racemic compound,² carries an electric polarization \mathbf{OO}' parallel to its director \mathbf{m}_1 . In this simple model, the x - y projection of the total polarization of an N -layer Sm- O^* film is given by \mathbf{OP}'_N , simply denoted as $\mathbf{P}(N)$ or \mathbf{P} hereafter. Notice that the points P_N and P'_N are equally spaced on two circles centered at Ω , and that they are gathered according to the parity of N . These features are a clear consequence of the alternate and helicoidal structure of the Sm- O^* phase. Assimilating the x - y plane to the complex plane, we calculate the x - y projection of the total polarization of the Sm- O^* film to be

$$\mathcal{P} = p_s + jp_{\parallel} + (-1)^{N-1} p'_s \exp[j\omega(N-1)] + p_b \{ [1 + (-1)^N \exp[j\omega(N-1)]] [1 + \exp(-j\omega)] / 2[1 + \cos\omega] - 1 \}, \quad (1)$$

where p_b is the ferroelectric polarization of a Sm- O^* layer in the bulk, p'_s is the ferroelectric polarization of the last layer in contact with the isotropic phase, p_s is the ferroelectric polarization of the first layer at the free surface, and p_{\parallel} is the x - y projection of its nonferroelectric polarization. From this calculation we thus deduce two experimental quantities: the modulus $P(N)$ of the x - y projection of the permanent electric polarization of the Sm- O^* film and the angle of this polarization relative to the director \mathbf{n} , which is

$$[\mathbf{P}, \mathbf{n}] = \tan^{-1} [\text{Im}(\mathcal{P}) / \text{Re}(\mathcal{P})] - \omega N / 2, \quad (2)$$

where the last layer has been taken equivalent to two smectic layers in the calculation of the director \mathbf{n} (see below). To first order in ω , this expression simply yields

$$\omega = 2(\alpha'_o \alpha'_e)^{1/2}, \quad (3)$$

where α'_o and α'_e are the derivatives of $[\mathbf{P}, \mathbf{n}]$ relative to N at $N=0$, for the odd and even cases, respectively.

The experimental procedure is the same as described in Ref. 2. A small quantity of chiral MHTAC is deposited on a clean and dried glass plate in the 2-mm interval between parallel gold electrodes. In reality, we do not take pure chiral MHTAC for this experiment because of the existence of a small domain of the smectic- Q phase in the pure compound¹ which prevents the observation of contact between the isotropic and smectic- O phases. To avoid this problem, we instead use a mixture of the two enantiomers: 95.25% (+ +) and 4.75% (- -). The sample is placed in a Mettler stage and observed in transmitted light with a polarizing Leica microscope. The Sm- O^* film of MHTAC, even a few layers thick, is not too difficult to observe as a result of the unusually large path differences of ≈ 0.5 nm per smectic layer between the ordinary and extraordinary rays in normal incidence.⁸ Moreover, the visibility of the film is noticeably improved when using a compensator of very small phase shift. The forming of a new smectic layer at the smectic-isotropic interface is then marked by a growing area of slightly different light intensity, well delimited by a tiny line. Starting from a high enough temperature where the film is not yet formed, and slowly decreasing

the temperature, we can thus observe and optically follow the layer-by-layer growth of the film. First, a nematic film of thickness approximately equivalent to two smectic layers² appears after a continuous transition, and persists until 141 °C. Then, with continued cooling of the sample, new smectic layers are separately generated at first-order layering transitions. They are preceded by transition fronts, which more specifically are simple surface dislocation lines. The process may be slowed down enough to allow correct counting of the number of the layers N in the film,⁹ and thus to determine its total thickness $(N+1)D$, $D=30$ Å being the thickness of the smectic layers.¹

The induced films floating on isotropic droplets, like free-standing films,¹⁰ are not anchored by any solid contact. They can thus be perfectly oriented by applying a horizontal electric field \mathbf{E} (i.e., parallel to them), except along 2π disclination walls where the director \mathbf{n} makes a complete rotation. These walls are useful in practice. They provide the first signature of the film at its very beginning, and because they often stick to the surface dislocation lines, they also help to observe the layering transitions, especially at low values of N . They are the physical consequence of the competition between the elastic energy and the coupling to the applied electric field.¹¹ As in the racemic Sm- O films,² the walls in the chiral Sm- O^* films are completely displaced on reversing \mathbf{E} . This demonstrates that the electric coupling is mainly due to a permanent polarization attached to the film, and more exactly to its horizontal projection \mathbf{P} onto the film. Neglecting the induced polarization and the space charge $\mathbf{V} \cdot \mathbf{P}$, and assuming one elastic constant K for the 2D film, the free energy of a wall reduces to

$$F = \int [\frac{1}{2} K (\mathbf{V} \cdot \mathbf{n})^2 - \mathbf{P} \cdot \mathbf{E}] dS.$$

The wall width, defined by the distance between the lines where \mathbf{n} is perpendicular to its asymptotic orientation far from the wall, is then given by¹¹

$$w = -2[K/PE]^{1/2} \ln \tan(\pi/8).$$

The measurements of the wall widths are performed

optically, using a rotating Leica compensator. They show, within 3% accuracy, that $\omega \propto E^{-1/2}$, which justifies the approximations made above in the calculations of ω , and therefore yield the ratio K/P of the Sm- O^* film. Simultaneously to this measurement, we determine the direction of extinction of the film between crossed polarizers. In our case where the film thickness is much smaller than the cholesteric pitch,¹² this measurement yields the direction of \mathbf{n} (mod $\pi/2$). The complete determination of \mathbf{n} is separately obtained with the compensator. We thus measure the angle $[\mathbf{P}, \mathbf{n}]$ between \mathbf{P} (directed along \mathbf{E} , i.e., along the normal to the electrodes, far from the walls) and \mathbf{n} . The measurements of $[\mathbf{P}, \mathbf{n}]$ and K/P are given in Fig. 2 as functions of N . Both of them display quite different behaviors depending on the parity of the number of layers in the film, N .

In particular, this means that the director \mathbf{n} of a Sm- O^* film submitted to a homogeneous electric field is oriented differently depending on the parity of N , and that, consequently, the two types of regions in the film with odd and even numbers of layers exhibit different grey colors when observed between crossed polarizers. Other parity effects also appear. For instance, the growth of a new smectic layer at the smectic-isotropic interface generates a surface dislocation line which often takes the shape of an arrow on applying an electric field. Remarkably, the directions of the arrows relative to \mathbf{E} depend on the parity of N also.¹³ All these parity effects complement the parity effects already observed in the racemic Sm- O , and strongly suggest the alternate or heringbone microscopic structure of the chiral and racemic Sm- O phases.

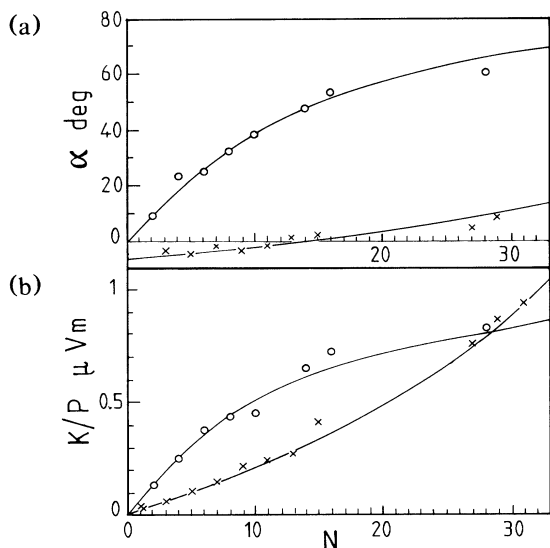


FIG. 2. Measurements of the horizontal projection \mathbf{P} of the electric polarization of the Sm- O^* film vs the number of its layers, N (crosses for odd N , circles for even N). The solid lines correspond to the theory (see text). (a) Angle $\alpha = [\mathbf{P}, \mathbf{n}] + (-1)^N \times 90$, in degrees, vs N . (b) Ratio K/P of the 2D elastic constant of the film over its projected polarization vs N .

The analysis of the data in Fig. 2 may be performed in a rather simple manner. Measuring the slopes at the origin in Fig. 2(a), and using Eq. (3), we first obtain the twist angle of the Sm- O^* film:

$$\omega = 3 \pm 0.1 \text{ deg}/(\text{smectic layer}).$$

With Eq. (2), we then deduce the polar angle of the polarization $\mathbf{P}(N)$ in the x - y plane for each measurement in Fig. 2(a). Taking $K = ND\mathcal{H} \sin^2\psi$,¹⁴ with $\mathcal{H} \sim 5 \times 10^{-7}$ cgs as the average Franck elastic constant, we also obtain the moduli $P(N)$ from the data of Fig. 2(b). The results are gathered in Fig. 3 which displays the x - y projections of the polarizations $\mathbf{P}(N)$ of N -layer Sm- O^* films. Clearly the points P_N thus obtained are spread on a circle within the experimental errors, and divided into two groups according to their parity. Notice that this experimental result is fairly consistent with the construction of Fig. 1(c). The center Ω of the circle is obtained by taking the middles of the segments $P_N P_{N+1}$. From the diameter of the circle, we determine $p_b - 2p'_s = 5.6 \times 10^6$ nC/cm, and from the coordinates of Ω we have $p_b - 2p_s = 3 \times 10^{-6}$ nC/cm and $p_{\parallel} - \frac{1}{2} p_b \sin(\omega/2) = 2.5 \times 10^{-7}$ nC/cm. Making the reasonable assumption that p_{\parallel} keeps the same value as in the racemic compound,² we find the following set of results for the layer polarizations of the Sm- O^* film expressed per surface unit: $p_{\parallel} = 3.8 \times 10^{-7}$ nC/cm, $p_s \approx 3.5 \times 10^{-6}$ nC/cm, $p'_s \approx 2 \times 10^{-6}$ nC/cm, and $p_b \approx 10^{-5}$ nC/cm.¹⁵ Because of error propagation, these last three results have large relative uncertainties, about 3 times that on p_{\parallel} .¹⁶ When inserted into Eq. (1), they yield the theoretical functions $(K/P)(N)$ and $\alpha(N)$ drawn as the solid lines in Fig. 2, without any further fitting.

The good agreement of this analysis with the experimental results (Figs. 2 and 3) naturally confirms the va-

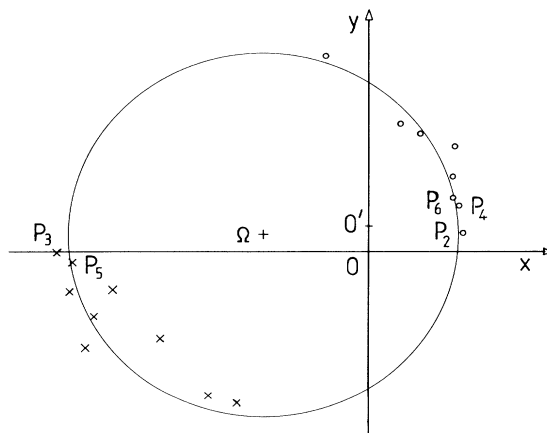


FIG. 3. Electric polarizations $\mathbf{P}(N)$ of Sm- O^* films of N layers, projected in the x - y plane (crosses for odd N , circles for even N). They correspond to the data common to both Figs. 2(a) and 2(b). Only the first polarizations are labeled. The values of N of the others may easily be deduced with the help of Fig. 2.

lidity of our model, and, first of all, provides a supplementary proof for the herringbone structure of Sm-O. Also, the simplified view of the film as a stack of identical Sm-O* layers, except for the two bordering layers at the interfaces, appears to be quite satisfactory within the experimental errors. It indicates a reduced antiferroelectric polarization in the two bordering layers of the film where the molecules, in contact with air and the isotropic phase, are less stabilized. Moreover, the anomalously weak polarization of the last layer compared to its thickness is consistent with the nematic nature of this layer.

Probably because the MHTAC molecule bears two chiral centers, the bulk antiferroelectric polarization p_b is relatively large, $p_b \approx 30$ nC/cm² when expressed per volume units, or $p_b \approx 0.1$ D per molecule, and the helicoidal pitch of the Sm-O* phase is remarkably short, $\Lambda = 0.36$ μm . Nevertheless, contrary to recent suggestions,⁴ these particular features cannot be invoked to explain the herringbone structure, just because the Sm-O* phase also exists at any dilution with the racemate, having then ordinary, and possibly vanishing, values for the antiferroelectric polarizations and pitches. Let us finally notice that the hypothesis of a 2D elastic constant K , proportional to the film thickness minus one smectic layer, is *a posteriori* justified by the agreement of the data with the circle in Fig. 3.

In conclusion, our macroscopic measurements of the electric polarization of the Sm-O* film directly prove its antiferroelectricity, and yield a new confirmation of the herringbone structure of the Sm-O phase. In this way, they contribute to a better understanding of this rather exotic phase, optically equivalent to a *chiral biaxial smectic-A* phase.

We wish to thank P. Keller and C. Germain for providing us with the MHTAC.

¹A. M. Levelut, C. Germain, P. Keller, L. Liébert, and J. Billard, *J. Phys. (Paris)* **44**, 623 (1983).

²Y. Galerne and L. Liébert, *Phys. Rev. Lett.* **64**, 906 (1990).

³Y. Galerne and L. Liébert, in *Proceedings of the Second International Conference on Ferroelectric Liquid Crystals*, Göteborg, Sweden, 1989 (to be published).

⁴H. Takezoe, A. D. L. Chandani, J. Lee, E. Gorecka, Y. Ouchi, A. Fukuda, K. Terashima, K. Furukawa, and A. Kishi, in *Proceedings of the Second International Conference on Ferroelectric Liquid Crystals* (Ref. 3); E. Gorecka, A. D. L. Chandani, Y. Ouchi, H. Takezoe, and A. Fukuda, *Jpn. J. Appl.*

Phys. **29**, 131 (1990), and references therein.

⁵A. M. Levelut, R. J. Tarento, F. Fardouin, M. F. Achard, and G. Sigaud, *Phys. Rev. A* **24**, 2180 (1981).

⁶B. Ocko, A. Braslau, P. Pershan, J. Als-Nielsen, and M. Deutsch, *Phys. Rev. Lett.* **57**, 94 (1986), and references therein.

⁷B. Swanson, H. Stragier, D. Tweet, and L. Sorensen, *Phys. Rev. Lett.* **62**, 909 (1989).

⁸The large path difference in normal incidence in the Sm-O phase of MHTAC is due to the exceptional association of a strong molecular tilt $\psi \approx 50^\circ$ with a large birefringence $\Delta n \approx 0.3$ along the molecules (see Ref. 2).

⁹Note that the definition of N is different here from that of Ref. 2 where the nematic layer was directly taken equal to two smectic layers in the counting.

¹⁰C. Young, R. Pindak, N. Clark, and R. Meyer, *Phys. Rev. Lett.* **40**, 773 (1978).

¹¹R. Pindak, C. Young, R. Meyer, and N. Clark, *Phys. Rev. Lett.* **45**, 1193 (1980).

¹²Y. Galerne (to be published).

¹³These arrows originate from the preferential anchoring of the director \mathbf{n} at an angle to the surface dislocation lines. \mathbf{n} can thus take two different anchoring directions along the line. The place where the anchoring direction is reversed sharply breaks the line, making the tip of an arrow. Also at this place, \mathbf{n} , and therefore \mathbf{P} , strongly diverges and produces an electric charge which orients the arrow in the electric field. In the Sm-O* films, due to chirality, the arrowheads exhibit hooked tips, and their two directions of orientation, according to the parity of N , do not coincide anymore with \mathbf{E} .

¹⁴This expression is slightly different from the expression used in Ref. 2. Here we directly take into account the observation (Fig. 3 in Ref. 2) that the 2D elastic constant in the floating films is proportional to the thickness of the film *minus* one smectic layer. Let us notice that such a behavior is consistent with an earlier observation by Rosenblatt *et al.* in free-standing films [C. Rosenblatt, R. Pindak, N. Clark, and R. Meyer, *Phys. Rev. Lett.* **42**, 1220 (1979)], that the smectic layers in contact with air, or more exactly at a distance smaller than the range of the interactions with air, have a reduced contribution to the 2D elastic constant, because their molecules undergo angular interactions with only a half space of the molecules.

¹⁵Let us notice that due to antiferroelectricity, the electric polarization of the Sm-O* film $P(N)$ remains of the order of magnitude of the polarization of one smectic layer, i.e., $\approx 10^{-5}$ nC/cm. This justifies the neglect of the space charge $\nabla \cdot \mathbf{P}$ and its consequences on the effective splay elastic constant (Rosenblatt *et al.*, Ref. 14), and therefore this elastic constant may be considered as approximately equal to the bend one.

¹⁶The experimental difficulty in the absolute determination of p_b , p_s , and p'_s is fundamentally due to antiferroelectricity which almost completely compensates the polarization from one layer to another.